Pergamon

Int. J. Heat Mass Transfer. Vol. 37, No. 6, pp. 997–1003, 1994

0017-9310/94 $6.00 + 0.00

0017-9310(93)E0001-W

Natural convection heat transfer from a vertical plate—I. Enhancement with gas injection

AKIRA T. TOKUHIRO† and PAUL S. LYKOUDIS

School of Nuclear Engineering, Purdue University, West Lafayette, IN 47907, U.S.A.

(*Received* 30 *October* 1992 *and in final form* 24 *September* 1993)

Abstract—A natural convection heat transfer experiment in mercury was conducted with gas injection in a vertical enclosure heated on one face at constant heat flux and cooled on the opposite face. Nitrogen gas bubbles were injected from a row of hypodermic tubes facing upwards along the face of the heated plate. The range of the applied heat flux was $370 \leqslant q'' \leqslant 16000$ W m^{-2}, which corresponds to a modified Boussinesq number range of $10^5 \leqslant Bo_x^* \leqslant 10^9$. The gas injection rate range was $0.9 \leqslant Q_g \leqslant 9.2$ cm^3 s^{-1}. Local heat transfer and void fraction measurements were made with thermocouple and double-conductivity probes, respectively. The measured heat transfer coefficient at low heat fluxes with gas injection, where the free convective flow was mostly laminar along the heated plate, was enhanced at least two-fold. In comparison, at higher heat fluxes, where the flow was predominantly turbulent, gas injection enhanced the heat transfer coefficient very little even at the highest injection rate. The overall enhancement in the heat transfer coefficient due to the bubble-induced turbulence is a collective action of both the induced liquid motion by the bubbles and the turbulence created in their trails. Void fraction measurements at both low and high heat fluxes indicated a three layer boundary layer structure distinct from the thermal boundary layer. The layers are: a single-phase inner layer next to the heated wall, a two-component layer where most of the bubbles reside, and an outer single-phase layer extending to the core of the cell. An analysis of our mercury heat transfer data with zero gas injection indicates that the transition to turbulence occurs at a Rayleigh number of about 2×10^7 rather than 10^9, the accepted value.

1. INTRODUCTION

NATURAL convection heat transfer has been extensively investigated in the past with a variety of geometries and heat transfer media.

There have been many reviews of natural convection heat transfer from vertical heated geometries for ordinary fluids by Ede [1], Ostrach [2], Gebhart [3], Catton [4], Churchill [5], Raithby and Holland [6], Jaluria [7] and Yang [8]. Natural convection in liquid metals is also of interest in nuclear engineering, e.g. liquid metal fast breeder reactors and liquid metal blankets of Tokamaks, and in metallurgical processing. Natural convection in liquid metals has been reviewed by Romig [9], Lykoudis [10], Viskanta [11], Kulacki *et al.* [12] and Reed [13] with and without the presence of an external magnetic field.

The classic natural convection problem of a heated vertical plate immersed in an infinite bath has been experimentally investigated in liquid metals. Past investigations relevent to the present work, because of their similarity in geometry and other experimental conditions, are those by Emery [14], Julian and Akins [15], Humphreys and Welty [16], Sheriff and Davies [17], and Uotani [18]. Emery [14] studied the influence of a magnetic field on natural convection heat transfer in mercury with the wall held at constant temperature. He provided non-magnetic heat transfer data and showed only fair agreement with a correlation intended for ordinary fluids ($Pr \geqslant 1$). Julian and Akins [15] studied laminar convection in mercury and showed agreement between analytical and experimental measurements up to a modified Grashof number of $Gr_x^* \sim 10^9$. Humphreys and Welty [16] also conducted experiments with mercury and verified Julian and Akins' correlation up to $Gr_x^* \sim 7 \times 10^{10}$, even in the presence of temperature fluctuations which they detected by hot-wire anemometry beginning at $Gr_x^* \sim 4 \times 10^9$. Sheriff and Davies [17] on the other hand experimented with sodium and noted a transition in the heat transfer data from laminar to turbulent natural convection at $Bo_x^* \sim 10^7$. They also reported that the bulk temperature was stratified. Finally, Uotani [18] in experiments with lead-bismuth eutectic verified the result of Humphreys and Welty up to $Bo_x^* \sim 3 \times 10^8$. He found that stratification enhanced the natural convection heat transfer.

Upon reviewing these works, it occurred to us that natural convection heat transfer could be enhanced with gas injection. In the chemical industry, bubble column reactors have long been used to control and augment reaction rates. Schürgel and Lücke [19] have reviewed bubble column reactors in bio-chemical engineering. Tamari and Nishikawa [20], in a detailed experiment of natural convection over a vertical heated plate, demonstrated that the heat transfer coefficient could be enhanced with gas injection. In this experiment, the investigators used up to three injectors in water and ethyl alcohol. They derived

† Address of author for correspondence: Paul Scherrer Institute, Würenlingen, CH-5232 Villigen PSI, Switzerland.

NOMENCLATURE

Bo_x	Boussinesq number, $g\beta\Delta Tx^3/\alpha^2$
Bo_x^*	modified Boussinesq number, $NuBo$
D_{ch}	bubble chord length [10^{-3} m or mm]
Gr_x	Grashof number, $g\beta\Delta Tx^3/\nu^2$
Gr_x^*	modified Grashof number, $NuGr$
k	thermal conductivity [W m^{-1} K^{-1}]
Nu_x	local Nusselt number, hx/k
Pr	Prandtl number, ν/α
Q	gas injection rate identifier, Section 3
Q_g	gas injection rate [cm^3 s^{-1} or 10^{-6} m^3 s^{-1}]
q''	heat flux rate [W m^{-2}]
Ra	Rayleigh number, $g\beta\Delta Tx^3/\alpha\nu$
T_w, T_∞	wall and bulk temperature [°C]
ΔT	wall to bulk temperature difference, $T_W - T_\infty$
V_{bub}	bubble rise velocity [m s^{-1}]
W	heat flux rate identifier, Section 3
X, Y, Z, x, y, z	coordinates.

Greek symbol

α	void fraction or thermal diffusivity [m^2 s^{-1}].

Subscripts and superscripts

bub	bubble
ch	chord length
g	gas
w	wall
x	indicates a local quantity along x-axis
0	signifies Nusselt-number without magnetic field
∞	bulk
$''$	indicates a quantity given as per unit area
*	*modified* quantity; based on q''.

an empirical heat transfer correlation that included parameters describing the spatial separation of the injectors from the heated wall and with each other. Subsequently at the Liquid Metal Thermal Hydraulics Laboratory of Purdue University, Wachowiak [21] verified that gas injection in water enhances the natural convection at least two-fold.

We have not been able to find any literature describing liquid metal natural convection with gas injection. We therefore set out to investigate this subject experimentally.

In the sections to follow, the experimental apparatus and experimental procedure will be described in Section 2. The experimental results are presented in Section 3. A discussion of results follows in Section 4 and a conclusion in Section 5.

2. EXPERIMENT

A schematic of the experimental apparatus is shown in Fig. 1. The apparatus measures 40 cm in height × 7 cm in width × 20 cm in depth (into the figure). The heated plate is 40 cm × 20 cm. The coordinate axes are as follows. The X- and Y-axes are, respectively, parallel and perpendicular to the heated wall while the Z-axis is into the figure. The origin is located at the bottom of the vertical midline over the width of the heated plate. There are 14 independently controlled heaters (Chromalox) attached to the heated wall (left) and a water-cooled jacket provides cooling to the opposite wall. There are 28 J-type thermocouples attached to the wall to measure the wall temperature. The lower portion of the cooled wall is tapered in accordance with a previous experiment by Papailiou [22]. In this experiment, Papailiou verified the existence of a similar solution developed by Lykoudis [23] for magneto-fluid-mechanic natural convection with a magnetic field intensity varying as $X^{-1/4}$. In this experiment the magnet was not used. Gas injection is provided by 11 equally-spaced hypodermic tubes (0.9

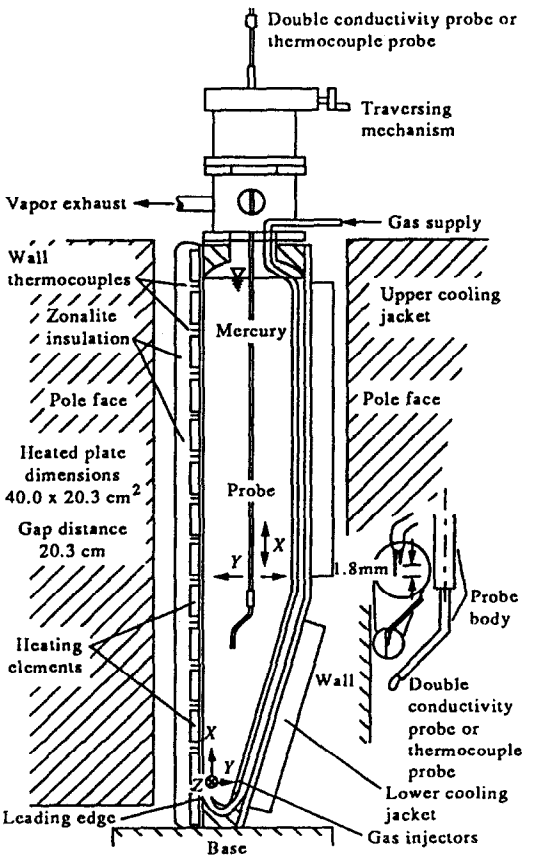

FIG. 1. Schematic of natural convection cell.

mm dia.), a distance $Y = 2$ mm from the wall. The placement of the tubes was based on the results of Tamari and Nishikawa [20]. Both the thermocouple probe (0.5 mm dia.) and double-conductivity probe (1.8 mm offset), respectively, are mounted on a traversing mechanism with movement in the Y-direction and inserted through a window located on top of the apparatus. The mercury used in the experiment is quadruply-distilled and the injected gas is high purity (99.995%) nitrogen.

The experiment was conducted by setting the wall heat flux at a predetermined level and adjusting the cooling rate so that the bulk temperature could be maintained near room temperature. This was done in order to minimize heat losses and to maintain a low volumetric concentration of mercury vapor in the laboratory. The bulk temperature was then monitored until a steady state condition was established. Once the bulk temperature ceased to fluctuate $\sim 0.5^{\circ}$C over a 40–60 min period, steady state was assumed to be attained. For laminar convection, this took 6–10 h, whereas for turbulent convection, 4–6 h. At this point the heater voltage, heater current, wall temperature and bulk temperatures were recorded. The raw temperature data were then curve-fitted with a polynomial equation using the Sigma-Plot [24] software package. After determining the local temperature difference across the thermal boundary layer and the input heat flux, the local Nusselt and modified Boussinesq numbers were calculated. The thermal properties were evaluated at the average bulk temperature. Further details of the apparatus and the experimental procedures are provided in Tokuhiro [25].

3. RESULTS

The local heat transfer data of previous experiments [14–18] are shown in Fig. 2 along with the laminar correlation. For clarity, only a selected number of data points from past investigations have been plotted in this figure. In some instances, the original data were presented in terms of the Rayleigh [14] or the modified Grashof number. These data were recast for the purpose of comparison in terms of the modified Boussinesq number. Recall that the Boussinesq number is the product of the Rayleigh and Prandtl numbers ($Bo = RaPr$) whereas the modified Boussinesq number is the product of the Nusselt and Boussinesq numbers ($Bo^* = NuBo$). The data in Fig. 2 represent natural convection without the influence of thermal stratification.

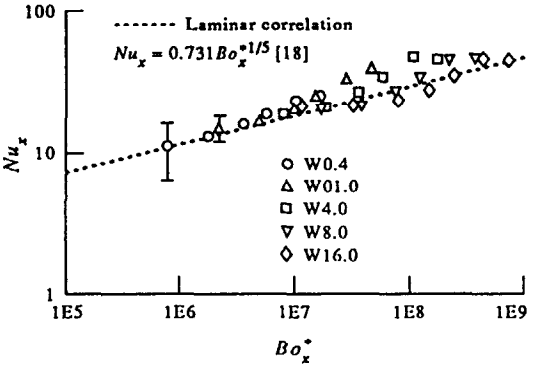

FIG. 3. Local heat transfer data, single-phase, at low and high heat fluxes.

The present local heat transfer results are shown in Fig. 3. In contrast to Fig. 2, the modified Boussinesq scale varies from 10^5 to 10^9 because our data points were taken in this range. Also in Fig. 3, the different heat fluxes are identified by W and later (starting with Fig. 4), in cases involving gas injection, by letter Q. In the text and figures, for quick recognition by the reader of a certain value of W and Q, we attach to each letter an up to three digit number indicating its value. The corresponding numerical value for each W

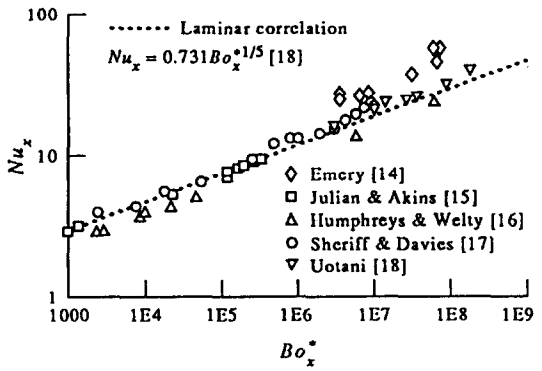

FIG. 2. Local heat transfer data of previous investigations.

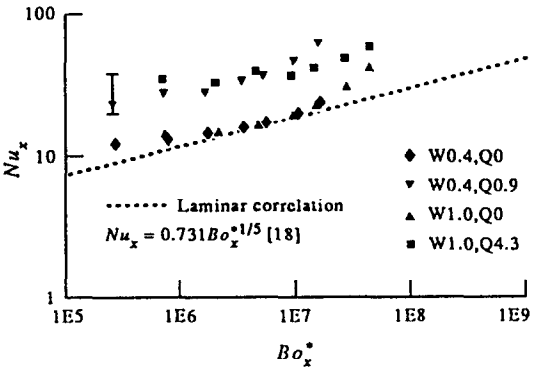

FIG. 4. Local heat transfer data at low heat fluxes W0.4 and W1.0 with gas injection.

Table 1. A guide to heat fluxes and gas injection rates used in the experiment

Heat flux rates, kW m^{-2}		
W0.4	represents	$q'' \sim 0.37$
W1.0		$q'' \sim 0.97$
W4.0		$q'' \sim 3.90$
W8.0		$q'' \sim 8.10$
W16.0		$q'' \sim 16.00$
Gas injection rates, cm^3 s^{-1}		
Q0.9	represents	$Q = 0.9$
Q2.1		$Q = 2.1$
Q4.3		$Q = 4.3$
Q9.2		$Q = 9.2$

and Q code is given in Table 1. Figure 3 shows our single-phase data at 'low' and 'high' heat fluxes. At low heat fluxes, the flow along the plate is mostly laminar while at high heat fluxes the flow is mostly turbulent.

In Figs. 4 and 5 we present the heat transfer data at low and high heat fluxes in the presence of gas injection. For the heat flux rate $W0.4$, only one injection rate $Q0.9$ was used. Here higher injection rates resulted in a $\Delta T(=T_w-T_b)$ too small to present with confidence. Error analysis revealed in this case that the error was as large as the measured ΔT. In each of the figures we present the representative error bar. For an error smaller than approximately 10%, the error bar is smaller than the datum symbol and is not visible.

In Figs. 6–8, we present a representative experimental chord length, bubble velocity and void fraction profile for the low and high heat fluxes, respectively. These measurements were taken with a double conductivity probe at an X-location 11 cm from the leading edge. This station is located at approximately one-third the length of the heated plate. The station represents a compromise between a location in which a statistically meaningful number of bubble events

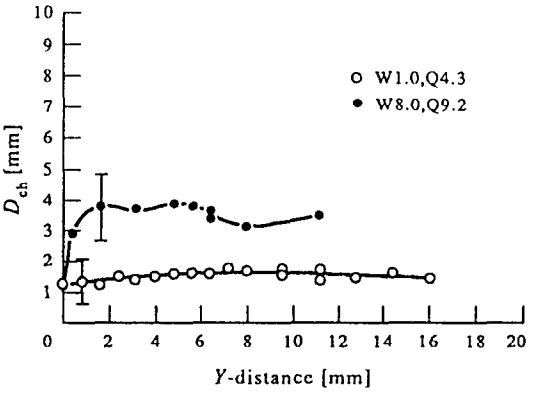

FIG. 6. Bubble chord length variation along the Y-axis with gas injection rate Q4.3 at heat flux W1.0 and gas injection rate Q9.2 at heat flux W8.0.

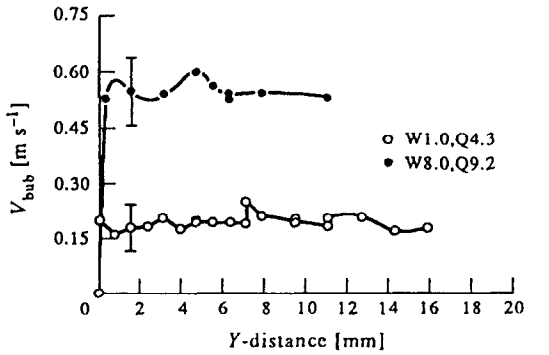

FIG. 7. Bubble rise velocity variation along the Y-axis with gas injection rate Q4.3 at heat flux W1.0 and gas injection rate Q9.2 at heat flux W8.0

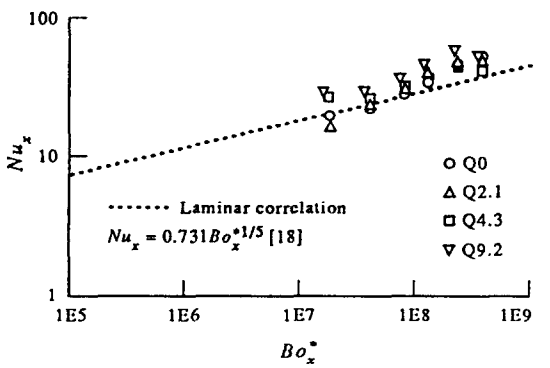

FIG. 5. Local heat transfer data at high heat flux W8.0 with gas injection.

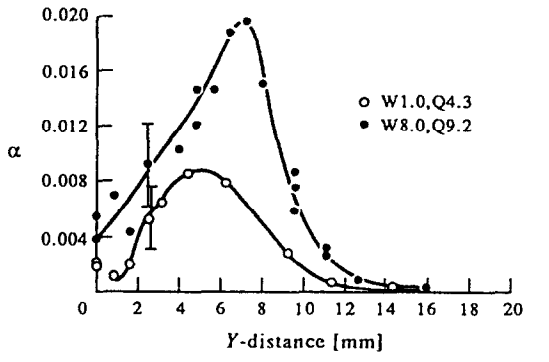

FIG. 8. Void fraction profile along the Y-axis with gas injection rate Q4.3 at heat flux W1.0 and gas injection rate Q9.2 at heat flux W8.0.

occur and a region where most of the heat transfer takes place. The curves shown were generated by using the Sigma-Plot software package.

4. DISCUSSION

4.1. *Single-phase data*

Figure 3 shows the heat transfer data taken in the laminar and turbulent natural convection regimes. This figure includes only the data obtained in the middle 20 cm of the test section thus, eliminating data that clearly show entrance and exit effects. However, these data are included and discussed in Tokuhiro [25]. For the heat fluxes W0.4 and W1.0, the points at low modified Boussinesq number follow the laminar theory and agree with the data produced by the previous investigators as shown in Fig. 2 up to approximately $Bo_x^* \sim 6 \times 10^6$, where a smooth transition to turbulent convection begins. This trend is similar to that of Sheriff and Davies [17]. The points beyond $Bo_x^* \sim 6 \times 10^6$ approximate the 1/3rd slope characteristic of turbulent convection. On the other hand, the data of Humphreys and Welty [16] and Uotani [18] follow the laminar correlation to approximately $Bo_x^* \sim 2 \times 10^8$. It should be noted, that Humphreys and Welty reported hot-film anemometry data from which they detect transition to turbulence at about the same modified Boussinesq number as we do. However, this transition is not reflected in their heat transfer data. Unfortunately, we do not have similar information in Uotani's work [18].

At this point we should bring into discussion that in our experiment we found the transition to turbulence to occur at approximately $Ra \sim 2 \times 10^7$ ($Bo^* \sim 6 \times 10^6$) rather than $Ra \sim 10^9$, the conventional accepted value. This lower transition Rayleigh number supports Bejan and Lage [26] who have suggested that low Prandtl number fluids have a lower transition to turbulent convection Rayleigh number. Bejan and Lage re-examined the transition criteria in the natural convection problem and argued with an order of magnitude analysis that the transition Rayleigh number criterion has a strong Prandtl number dependence for all fluids. In fact, the emerging criterion is that for all fluids, $Gr = 10^9$, correlates all transition data, including ours since for mercury with $Pr = 0.02$ and $Ra \sim 2 \times 10^7$, $Gr = 10^9$.

In Fig. 3, one can see that for heat fluxes above W1.0, the Nusselt number not only depends on the modified Boussinesq number but also on the heat flux rate W. On the other hand, the stratified heat transfer data indicate that for a given wall heat flux, the slope of the Nusselt number vs the Boussinesq number remains the same as with the non-stratified data. We attribute this trend to the stratification we observed when the bulk temperature gradient in the X-direction increased with increasing heat flux. We have considered the influence of stratification separately and present the result of our analysis in a separate paper.

4.2. *Data with gas injection*

In the laminar regime, where $Bo_x^* \leqslant 6 \times 10^6$, the wall to bulk temperature difference for zero gas injection is approximately 1.5°C. For our lowest injection rate of Q0.9, the measured difference was about 0.50–0.75°C or less. Smaller temperature differences were difficult, if not impossible to measure considering the inherent fluctuations of the wall temperature and associated error in ΔT. Even so, at the rate of Q0.9, we measured an enhancement in the heat transfer coefficient of two to three times the single-phase result as shown in Fig. 4. This was also observed at the heat flux W1.0 with injection rate Q4.3 for all but the three uppermost points for which $Bo_x^* \geqslant 10^7$. On the other hand beyond 10^7, the relative enhancement in the heat transfer coefficient begins to decrease. These trends can be explained as follows. In the laminar natural convection regime, where the thermal boundary layer is fairly thick (~20–25 mm), the presence of the bubbles induces turbulence within the thermal boundary layer which dramatically enhances the heat transfer mechanism. This bubble-induced turbulence, the result of which we observe as an overall enhancement in the heat transfer coefficient, is a collective action of both the induced liquid motion by the bubbles and the turbulence left in their trails. In contrast, in the turbulent regime, the thermal boundary layer is thinner (~5–10 mm) and fewer bubbles reside within this layer; there are more bubbles exterior to the thermal boundary layer. Hence, the heat transfer coefficient is only moderately enhanced. These bubbles, however, suppress the bulk temperature gradient in the core region. This mitigates the influence due to stratification. There is thus a less pronounced change in local Nusselt number. The temperature profiles that verify the thermal boundary layer thickness at low and high fluxes are given in ref. [25].

In Fig. 5 we show the data at a high heat flux rate W8.0 for three different injection rates. Similar results were obtained at the heat flux rates W4.0 and W16.0 but are not shown here. They are included in ref. [25]. At the injection rates Q2.1 and Q4.3, we see no appreciable heat transfer enhancement. This is consistent with the trend shown for the heat flux rate W1.0 with the injection rate Q4.3 where the upper three points were in the turbulent regime. On the other hand, we do observe a small enhancement of about 20–25% at the highest injection rate Q9.2. Here it appears likely that the small increase in the Nusselt number is due to the high density of bubbles, a few of which probably penetrate the thin turbulent boundary layer.

4.3. *Void-related measurements*

The physical model of the enhancement mechanism is equally supported by void-related measurements at low and high heat flux. In Figs. 6–8 we show bubble chord length, bubble rise velocity and void fraction profiles, respectively. In these figures we show data

for two cases, one for laminar (W1.0, Q4.3) and one for turbulent (W8.0, Q9.2).

Figure 6 shows that the bubble size is nearly constant through the two-phase boundary layer. These bubble sizes were approximately verified with the information provided in Wallis [27] which predicts a bubble size range, $3.9 \leqslant D_{ch} \leqslant 6.0$ mm, corresponding to the minimum and maximum gas injection rate. More importantly, we note that the bubble size is smaller than the thermal boundary layer thickness ($\sim$20–25 mm) at low heat flux while at high heat flux, the bubble size is of the same order as the thermal boundary layer ($\sim$5–10 mm). This indicates that the heat transfer enhancement at low heat flux is due to the bubble-induced turbulence within the thermal boundary layer.

The bubble rise velocities shown in Fig. 7 were also verified with a bubble rise velocity correlation contained in Wallis [27]. At low heat fluxes an approximation for a single bubble rising in a stagnant pool was used and gave a value of 34 cm s^{-1} as compared to the measured $\sim$30 cm s^{-1}. The agreement is not surprising since the void fraction is very small (one bubble event per second) and the convective velocity is also small ($\leqslant$ 1 cm s^{-1}) according to Peinecke and Welty [28]. At high heat fluxes, however, the same velocity correlation cannot be expected to accurately predict the measured rise velocities because the conditions of the correlation are not fulfilled. In this case we expect a larger rise velocity because first the bubbles are swept upwards by the recirculating flow from the bottom of the cell and second, as reported by Sano and Mori [29], the rise velocity increases proportionally to the void fraction up to $\alpha \sim 1\%$. At high heat fluxes we had more than one bubble event per second and equally a larger void fraction than at low heat fluxes. In an experiment by Lykoudis *et al.* [30] using mercury, gas was injected from the inner cylinder of a vertical set of concentric cylinders. The inner cylinder was suspended by the outer cylinder so that flow recirculated near the point of gas injection from the outer annulus to the inner cylinder. At a void fraction of 1% and mean liquid velocity of 35 cm s^{-1}, their measured bubble rise velocity was 65 cm s^{-1}. Since their physical situation is similar to ours, the approximate agreement between their measured bubble velocity and the present bubble velocity provides a qualitative verification of the bubble rise velocity at the high heat flux rate.

In Fig. 8 we show void fraction measurements. As is noted in detail in ref. [25] when the local void fraction at a station X is integrated through Y, one does not recover the volume corresponding to the injected rate. This is attributed to the fact that there seems to be considerable dispersion in the Z-direction for which no measurements were made.

It should be clear that more experiments should be conducted to determine the bubble parameters with more precision in order to fully clarify the influence of bubble geometry and dynamics on heat transfer.

5. CONCLUSIONS

An experimental investigation of laminar and turbulent natural convection heat transfer from a vertical plate in mercury with gas injection was undertaken. The experiment was conducted with the plate held at constant heat flux. Gas was injected at the bottom of the heated section. Local heat transfer and void measurements (bubble chord length, bubble rise velocity and void fraction) were taken. At the higher heat fluxes, stratification was observed.

Our single-phase measurements verified the laminar data of previous investigators for $Bo_x^* \leqslant 6 \times 10^6$, beyond which the Nusselt number showed a trend characteristic of turbulent convection influenced by stratification. With the injection of gas, the heat transfer coefficient was enhanced two- to three-fold for the low heat fluxes. On the other hand, this enhancement was less pronounced at high heat fluxes with only a small augmentation observed at the highest injection rate. These trends were explained as follows. In the low heat flux cases, the presence of bubble-generated turbulence inside the relatively thick thermal boundary layer enhances the heat transfer process. In contrast at high heat fluxes, most of the bubbles appear outside the thinner thermal boundary layer. As a result, the injected bubbles do not contribute to the enhancement mechanism. These bubbles instead mitigate the stratification in the core region and suppress the influence of stratification on the heat transfer enhancement.

The void measurements supported our physical model of the enhancement mechanism. The void profile first indicated that most of the bubbles reside in a two-phase boundary layer in between an inner and outer single-phase layer. The inner layer is adjacent to the heat wall and the outer layer extends to the core region. Bubble chord length measurements showed that at low heat fluxes, the bubble sizes were smaller than the thermal boundary layer thickness. This supports the view that the heat transfer coefficient is thus enhanced by the bubble-induced turbulence in this layer. On the other hand, at high heat fluxes, the bubbles are nearly the same size as the thermal boundary layer thickness. These bubbles, therefore, cannot penetrate the thermal boundary layer to enhance the heat transfer process. They, however, contribute to the suppression of the stratification in the core region.

We should also bear in mind that the overall enhancement in the heat transfer coefficient due to the bubble-induced turbulence is a collective action of both the induced liquid motion by the bubbles and the turbulence created in their trails. It was not possible based on our measurements to identify the individual contributions of each of these factors.

Finally, we recognize at this point that the bubble parameters are difficult to determine with precision using one double-conductivity probe as we did. It is, therefore, recommended that, in order to further elucidate the influence of bubble dynamics on heat transfer, a multiple number of probes be used.

Acknowledgements—The authors would like to express their appreciation to the National Science Foundation who supported the research under Grant No. 8304743.

REFERENCES

1. A. J. Ede, Advances in free convection. In *Advances in Heat Transfer* (Edited by J. P. Hartnett and T. F. Irvine, Jr.), Chap. 1. Academic Press, New York (1967).
2. S. Ostrach, Natural convection in enclosures. In *Advances in Heat Transfer* (Edited by J. P. Hartnett and T. F. Irvine, Jr.), Chap. 3. Academic Press, New York (1972).
3. B. Gebhart, Natural convection flows and stability. In *Advances in Heat Transfer* (Edited by J. P. Hartnett and T. F. Irvine, Jr.), Chap. 4. Academic Press, New York (1973).
4. I. Catton, Natural convection in enclosures, *6th Int. Heat Transfer Conf.*, Toronto, Vol. 6, pp. 13–46 (1978).
5. S. W. Churchill, Free convection around immersed bodies. In *Single-Phase Convective Heat Transfer*, pp. 2.5.7-1–2.5.7-30. Hemisphere, New York (1983).
6. G. D. Raithby and K. G. Holland, Natural convection. In *Heat Transfer Fundamentals* (Edited by W. M. Rohsenow, J. P. Hartnett and E. N. Ganić), Chap. 6. McGraw-Hill, New York (1985).
7. Y. Jaluria, Basics of natural convection. In *Handbook of Single-Phase Convective Heat Transfer* (Edited by S. Kakaç, R. K. Shah and W. Aung), Chap. 8. Wiley, New York (1987).
8. K. T. Yang, Natural convection in enclosures. In *Handbook of Single-Phase Convective Heat Transfer* (Edited by S. Kakaç, R. K. Shah and W. Aung), Chap. 13. Wiley, New York (1987).
9. M. F. Romig, The influence of electric and magnetic fields on heat transfer to the electrically conducting fluids. In *Advances in Heat Transfer* (Edited by J. P. Hartnett and T. F. Irvine, Jr.), Chap. 5. Academic Press, New York (1964).
10. P. S. Lykoudis, Natural convection of electrically conducting fluids in the presence of magnetic fields. In *Natural Convection—Fundamentals and Applications* (Edited by S. Kakaç, W. Aung and R. Viskanta), pp. 1100–1117. Hemisphere, New York (1985).
11. R. Viskanta, Electric and magnetic fields. In *Handbook of Heat Transfer Fundamentals* (Edited by W. M. Rohsenow, J. P. Hartnett and E. N. Ganić), Chap. 10. McGraw-Hill, New York (1985).
12. F. A. Kulacki, J. Davidson and P. Dunn, Convective heat transfer with electric and magnetic fields. In *Handbook of Single-Phase Convective Heat Transfer* (Edited by S. Kakaç, R. K. Shah and W. Aung), Chap. 9. Wiley, New York (1987).
13. C. B. Reed, Convective heat transfer in liquid metals. In *Handbook of Single-Phase Heat Transfer* (Edited by S. Kakaç, R. K. Shah and W. Aung), Chap. 8. Wiley, New York (1987).
14. A. F. Emery, The effect of a magnetic field upon the free convection of a conducting fluid, *Trans. A.S.M.E., J. Heat Transfer*, 119–124, May (1963).
15. D. V. Julian and R. G. Akins, Experimental investigations of natural convection heat transfer to mercury, *Ind. Engng Chem. Fund.* **814,** 641–646 (1969).
16. W. W. Humphreys and J. R. Welty, Natural convection with mercury in a uniformly heated vertical channel during unstable laminar and transitional flow, *Am. Inst. Chem. Engng J.* **121,** 268–274 (1975).
17. N. Sheriff and N. W. Davies, Sodium natural convection from a vertical plate, *6th Int. Heat Transfer Conf.*, Toronto, Vol. 6, NR-23, pp. 131–136 (1978).
18. M. Uotani, Natural convection heat transfer in thermally stratified liquid metal, *J. Nucl. Sci. Technol.* **24**(6), 442–451 (1987).
19. K. Schürgel and J. Lücke, Bubble column bioreactors. In *Advances Biochemical Engineering* (Edited by T. Ghose, A. Fiechter and N. Blakebrough), Chap. 1. Springer, Berlin (1977).
20. M. Tamari and K. Nishikawa, The stirring effect of bubbles upon the heat transfer to liquids, *Jap. Res.—Heat Transfer* **5**(2), 31–43 (1976).
21. R. M. Wachowiak, The enhancement of natural convection by rising bubbles, M.S. Thesis, Purdue University, West Lafayette, Indiana (1986).
22. D. D. Papailiou and P. S. Lykoudis, Magneto-fluid-mechanics laminar natural convection—An experiment, *Int. J. Heat Mass Transfer* **11,** 1385–1391 (1968).
23. P. S. Lykoudis, Natural convection of an electrically conducting fluid in the presence of a magnetic field, *Int. J. Heat Mass Transfer* **5,** 23–34 (1962).
24. Sigma-Plot (Trademark), Version 3.1, Jandel Scientific, Sausalito, CA (copyright 1987).
25. A. Tokuhiro, Natural convection heat transfer enhancement in mercury with gas injection and in the presence of a magnetic field, Ph.D. Thesis, Purdue University, West Lafayette, Indiana (1991).
26. A. Bejan and J. L. Lage, The Prandtl number effect on the transition in natural convection along a vertical surface, *A.S.M.E. J. Heat Transfer* **112,** 787–790 (1990).
27. G. B. Wallis, *One-dimensional Two-phase Flow*, pp. 243–251. McGraw-Hill, New York (1969).
28. D. R. Peinecke and J. R. Welty, Velocity measurements for buoyancy-induced flow in mercury adjacent to vertical single cylinders, *Trans. A.S.M.E.*, 146–148, February (1976).
29. M. Sano and K. Mori, Dynamics of bubble swarms in liquid metals, *Trans. I.S.I.J.* **20,** 668–674 (1980).
30. P. S. Lykoudis, S. T. Revankar and D. B. Black, Turbulence in the presence of a magnetic field, unpublished (1989).